



*Dedicated to Professor Alexandru T. Balaban
on the occasion of his 80th anniversary*

MODELS OF THE ALGISTATIC ACTIVITY OF 5-AMINO-1-ARYL-1H-TETRAZOLES

Maria MRACEC,^{a,*} Tudor I. OPREA^{a,b} and Mircea MRACEC^a

^a Molecular Forecast Research Center, str. Prof.Dr. A. Păunescu-Podeanu Nr. 125, A 4, RO-300569 Timișoara, Roumania

^b Division of Biocomputing, University of New Mexico School of Medicine, Albuquerque, NM 87131, USA

Received November 30, 2010

Models for the algistatic activity of substituted 5-amino-1-aryl-1H-tetrazoles were obtained with the CoMFA (Comparative Molecular Field Analysis) and MTD (minimum topological difference) methods. Both methods agree with respect to the detrimental and beneficial regions of the substituents. The CoMFA model ($Q^2_{\text{LOO}} = 0.638$, $\text{see} = 0.342$, 3 latent variables) highlights the importance of steric, rather than electrostatic, interactions. A bi-parametric model, MTD, $\log P$ (where $\log P$ is the experimental n-octanol/water partition coefficient) stresses the importance of hydrophobicity over steric and electrostatic interactions ($Q^2_{\text{LOO}} = 0.958$; $\text{see} = 0.098$). Based on this QSAR study, we proposed a probable way of action of the algistatic derivatives from this series. Their hydrophobicity, steric and electronic properties allow these derivatives to act via their transport into membranar protein sites of some easy substitutable quinones. The presence of these aryltetrazoles with electron acceptor properties in the quinone's sites might disturb the chain of electron transfer in algae photosynthesis.

INTRODUCTION

The class of 1-aryltetrazolic derivatives contains compounds with a large spectrum of medicinal properties. They have anti-inflammatory, anti-arthritic, analgesic, coccidiostatic, antiviral or tuberculostatic effects.¹ A series of 20 derivatives of 5-amino-1-aryl-1H-tetrazole were shown to act as algistatics against *Chlorella vulgaris* cultures.¹ A QSAR study on this series was published in 2001 by Katritzki *et al.*² They used the CODESSA software for geometry optimization, descriptor calculation and variable selection. According to their QSAR models the algistatic activity of 1-aryl-tetrazoles is influenced by steric (shape, volume) and electronic descriptors. However, from the QSAR model obtained by Schelenz¹ resulted that the algistatic activity of 1-aryl-1-tetrazolyl derivatives strongly correlates with the experimentally determined n-octanol/water partition coefficient, $\log P$. Both results prompted us

to find out how important is the contribution of hydrophobicity, steric and electronic properties to the algistatic activity of 1-aryl-1-tetrazolyl derivatives.

For this purpose we used a 3D-QSAR method: Comparative Molecular Field Analysis,³ (CoMFA) and a 2D method: Minimum Topological Difference,⁴ (MTD). CoMFA is a molecular interaction fields⁵ method that highlights where alterations in the 3D structure are likely to correlate with biological variations in the target, *i.e.*, algistatic property. However, CoMFA is known to be conformer and alignment dependent.⁶ Therefore, we have also investigated this problem by applying a conformer-independent method, MTD. The MTD hypermolecule does require, however, an alignment. Furthermore, when models contain aside MTD other descriptors, through the optimization process MTD can change its physical significance. For example, to uncover steric effects, MTD must be optimized together with descriptors that can extract electronic and

* Corresponding author: mmracec@acad-icht.tm.edu.ro

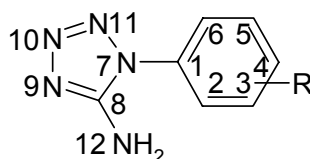
hydrophobicity information. This series allows to demonstrate this peculiarity of MTD.

METHODS

The structures of the 1-tetrazolyl derivatives are shown in Table 1. The 3D conformers for CoMFA analysis were obtained with CORINA.^{7,8}

Superimposition was performed on the largest active derivative **1** using the atoms 1, 6, 10, 12 (Table 1). CoMFA analyses, including Projections to Latent Structures, PLS,⁹ were carried out in SYBYL.¹⁰ Cross-validation,¹¹ using one derivative, leave-one-out (LOO) was applied.

Table 1
Structure, algistic activity (logA), hypermolecule vertex's occupancy ($x_{ij}=1$)
and values of significant descriptors for algistic activity



	R	logA	$x_{ij}=1$	logP	θ	q_2	MTD1	MTD2	MTD3
1	3,4-(CH) ₄	4.01	1-4	2.084	43.69	-0.127	3	4	2
2	3,4-Cl ₂	3.84	1,4	2.064	43.01	-0.134	5	6	4
3	3-Cl,4-Me	3.76	1,4	1.891	43.87	-0.135	5	6	4
4	4-OEt	3.31	3-5	1.315	46.03	-0.103	4	5	3
5	3-Cl	3.21	1	1.440	43.66	-0.140	6	7	5
6	4-Me	3.15	4	1.198	44.53	-0.134	6	7	4
7	2,5-Cl ₂	3.11	6,7	1.606	62.92	-0.078	7	8	6
8	3-Me	3.09	1	1.236	44.56	-0.144	6	7	5
9	2,3-(CH) ₄	3.07	1,6,8,9	1.715	62.37	-0.034	8	9	6
10	4-NO ₂	3.01	3,4,10	0.770	40.26	-0.159	4	5	2
11	2,5-Me ₂	2.98	1,11	1.455	131.15	-0.042	7	6	6
12	3-OMe	2.92	1,2	0.962	42.7	-0.219	5	6	4
13	3-NO ₂	2.79	1,2,9	0.669	41.76	-0.091	5	6	3
14	3-F	2.66	1	0.909	42.85	-0.185	6	7	5
15	H	2.65	-	0.688	44.51	-0.139	7	8	5
16	4-F	2.49	4	0.752	44.49	-0.113	6	7	4
17	2-Me	2.46	11	0.930	131.44	-0.037	8	7	6
18	2-Cl	2.40	6	0.870	62.81	-0.074	8	9	6
19	4-OH	2.19	4	0.326	45.77	-0.102	6	7	4
20	2-OMe	2.08	6,8	0.562	53.95	0.068	9	10	7

logA – algistic activity expressed as $-\log C_{50}$ (ref. 1); $x_{ij}=1$ – occupancy of vertices “j” of hypermolecule by the atoms of molecule “i”; logP (hydrophobicity descriptor) – experimental n-octanol/water partition coefficient (see ref. 1), θ (steric descriptor) – dihedral angle between the phenylic and tetrazolic rings; q_2 (electronic descriptor) – net charge on the C₂ atom in the phenyl ring; MTD1 – the MTD values resulted by MTD optimization with logP; MTD2 – the MTD values resulted by MTD optimization with logP and dihedral angle between phenylic and tetrazolic rings; MTD3 – the MTD values resulted by MTD optimization with logP and net charge on C2 atom of the phenylic ring

MTD_i, the MTD value for the “ith” molecule from the series was calculated with the relation:

$$MTD_i = s + \sum_{j=1}^M \epsilon_j x_{ij}$$

where s represents the number of vertices with $\epsilon_j = -1$ of a “standard” molecule; the “standard” can be the most active compound or a generic molecule which contains predominantly atoms or groups of atoms from most active structures; $j = 1 \dots M$ is the number of vertices in a hypermolecule resulted through the maximum

superposition, atom by atom of all molecules in the series; ϵ_j is a vector which can take the values 1 (detrimental vertices), 0 (irrelevant vertices) or -1 (beneficial vertices); x_{ij} is an index which represents the occupancy of the hypermolecule vertices ($x_{ij} = 1$ for occupied and $x_{ij} = 0$ for unoccupied vertices). The assignment of ϵ_j values is a cyclic process that ends when the best correlation coefficient is obtained for the equation:

$$A_i = a + a_1X_{i1} + a_2X_{i2} + \dots - b \text{ MTD}_i$$

X_{i1}, X_{i2}, \dots are other descriptors, the 'a' and 'b' values are the regression coefficients.

For 1-tetrazolyl derivatives a hypermolecule with $j=11$ vertices was obtained through atom by atom maximum superposition of molecules in the series. Initial "standard" was a generic molecule chosen by assigning as beneficial ($\epsilon_j = -1$) the vertices 1-5 occupied mainly in the first five most active molecules, and by assigning as detrimental ($\epsilon_j = 1$) the vertices 7 and 9 occupied mainly in the five least active derivatives.

Gas phase equilibrium geometries were optimized with the AM1 hamiltonian,¹² implemented in the HyperChem7.52 package.¹³ Optimization was performed with the Polak-Ribiere conjugate gradient algorithm using as stop criteria a RMS gradient of 0.01 kcal/Åmol and SCF convergence of 10^{-5} . All optimized geometries have $v_{\min} > 0$.

A series of electronic and steric descriptors: net atomic charges on the phenylic and tetrazolic rings, energies of the highest occupied molecular orbital and of the lowest unoccupied molecular orbital, chemical hardness,¹⁴ absolute electronegativity,¹⁴ dipole moment, and dihedral angle $C_2-C_1-N_7-C_8$ (θ) between the planes of the tetrazolic and phenylic

rings, molar refractivity, van der Waals area and volume, and solvent accessible surface area and solvent-accessible surface-bound molecular volume were obtained based on the optimized AM1 geometries. Electrotopological state indices were calculated according to the relation of Kier and Hall.¹⁵

RESULTS AND DISCUSSION

CoMFA analysis

The algistic activity, $\log A$, expressed as the reciprocal value of the isoeffective concentrations C_{50} , determined by Schelenz from photometrical measurements,¹ is shown in Table 1 and the CoMFA results are summarized in Table 2. The 3-component model was selected by applying the parsimony principle (less is better). Cross-validation method indicates a significant PLS model.¹⁰ The non-crossvalidated model is at the bottom of the Table 2.

The steric field interactions are shown in Figs. 1a and 1b for the highest and the lowest active molecules in the series, respectively. Steric fields indicate that 3-, 4- substitution at the (1-tetrazolyl)-phenyl moiety are beneficial for the activity. This is confirmed by the activity of beta-naphthyl in derivative (1) and 3,4-di-chloro in derivative (2). Lack of occupancy in the above region in derivative (15), as well as occupancy in other regions (2-methoxy in derivative (20)), appears to be detrimental for the algistic activity.

Table 2

Models obtained with CoMFA method					
	PC1	PC2	PC3	PC4	PC5
q^2_{LOO}	0.120	0.534	0.638	0.714	0.757
$P(q^2_{\text{LOO}}=0)$	0.853	0.039	0.008	0.002	0.001
SEP_{LOO}	0.502	0.376	0.342	0.314	0.299
R^2			0.946		
F			93.614		
$P(R^2=0)$			0		
SEE			0.132		

q^2_{LOO} – squared cross-validated correlation coefficient leave one out (LOO); F – Fisher test; P – chance correlation probability; SEP – the standard error of predictions; SEE – standard error of the estimate.

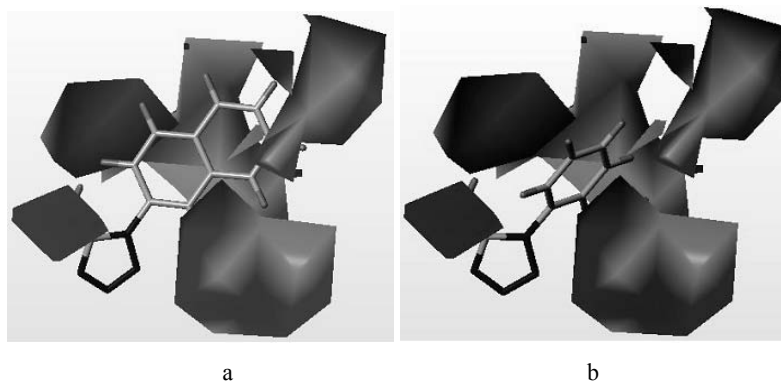


Fig. 1 – a) Derivative **1** ($\log A = 4.01$); b) derivative **20** ($\log A = 2.08$); shown in black and dark grey: 85% contribution of the stdev · coeff steric field favored areas; shown in light grey: 15% contribution of the stdev · coeff steric field unfavored areas

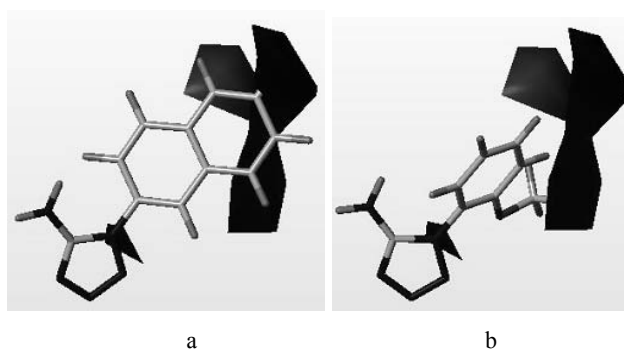


Fig. 2 – a) Derivative **1** ($\log A = 4.01$); b) derivative **20** ($\log A = 2.08$); shown in black: 85% contribution of the stdev · coeff electrostatic field favored areas; shown in dark grey (up left lateral zone): 15% contribution of the stdev · coeff electrostatic field unfavored areas.

The electrostatic field interactions are displayed in Figs. 2a and 2b, also for the highest and the lowest active molecules in the series. Electrostatic fields suggest that nonpolar substituents at the 3-, 4- positions of the 1-tetrazolyl-phenyl moiety are beneficial. This is confirmed by the activity of beta-naphthyl (derivative **1**) and 3,4 di-chloro (derivative **2**), compared to 3-nitro (derivative **13**) and 4-nitro (derivative **10**). Lack of occupancy in the above region, as well as occupancy in other regions, appears to have no influence for the activity. Steric field is dominant, 77% vs. 23% for the electrostatic field.

MLR analysis

The values of the most important properties for the algistatic activity are shown in Table 1. To find out if beside hydrophobicity ($\log P$) other properties (steric and/or electronic) have relevance for the algistatic activity, different mono- and multiple linear regressions (MLR) have been tested. Statistical indices for the most significant descriptors in

monoparametric regressions suggest that the hydrophobicity ($\log P$) is the dominant factor in the algistatic activity of 1-aryl-1-tetrazolyl derivatives.

In Table 3, where the statistical indices for five of the best bi- and three-parametric models are presented, the last three regressions contain the MTD descriptor which can encode steric, hydrophobicity or electronic information.

The optimized receptor map for model (3) ($\log P$, MTD) is shown in Fig. 3. It has three detrimental vertices (6, 8 and 11) and seven beneficial vertices (1-5, 7, 10). The detrimental vertices correspond to substituents attached at the 2-position of the phenyl ring, while the beneficial vertices are situated in a region starting from the 3-position of the phenyl ring. This result is in agreement with the CoMFA results regarding the beneficial and detrimental regions around the phenyl ring. In model (3) the MTD descriptor has a mixed content, both steric and electronic. To get reliable information on the actual physical meaning of MTD, in models (4) and (5) the Randić orthogonalization¹⁶ of scaled (0-1) descriptors was

applied. By scaling and orthogonalizing one can directly compare the content of steric or electronic information of the MTD descriptors in models (4) and (5). The order of descriptors and the partial correlation coefficients of the regressions resulted after the Randić orthogonalization are shown in Table 4.

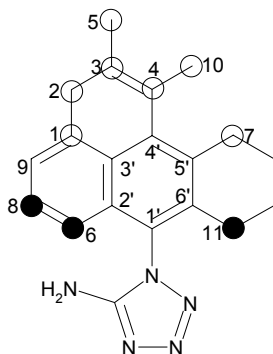


Fig. 3 – Hypermolecule, the numbering of its vertices and the representation of the optimized receptor map that contains seven beneficial vertices (open circles) and three detrimental vertices (black circles) for model logP, MTD. (Note that the hypermolecule vertices are numbered in the order of their occupancy by different atoms of molecules in the series ordered by their algistic activity).

By Randić orthogonalization¹⁶ of descriptors in the order logP, θ , MTD, the logP descriptor extracts from θ and MTD all hydrophobicity content and θ extracts from MTD all steric content leaving MTD with a pure electronic content. In the same manner Randić orthogonalization of descriptors in the order logP, q_2 , MTD, extracts from MTD hydrophobicity and electronic content and leaves MTD with a pure steric content. Examining the partial correlation coefficients in Table 4 one can see that the most important contribution to algistic activity comes from hydrophobicity and in a smaller extent from the electronic and steric properties of 1-aryl tetrazoles. Data in Table 4 suggest that the electronic and steric properties have approximately equal importance to algistic activity.

Comparing the significance of fields from CoMFA models with the significance of the descriptors resulted from MLR models one can suppose that CoMFA steric field may have a high hydrophobicity content. We suppose also that in Katritzki's models² the steric descriptors may also encode a large content of hydrophobicity which could be revealed by the descriptor orthogonalization.

From models (1) - (5) it results that compounds with high algistic activity should have

substituents with high hydrophobicity. These substituents should be bound in positions 3- and/or 4- of the phenyl ring. The higher negative charge on the C₂ atom from the phenylic ring, the highest the algistic activity. Models (1) - (5) and the optimized receptor maps from MTD models allow to imagine other compounds with potential high activity, as for example the compounds in Table 5. The values of different descriptors obtained using the optimized AM1 geometries of the derivatives I-V, as well as the logA values estimated using models (1) - (5) are shown in Table 5.

The properties of tetrazolic derivatives important for the algistic activity allow some hypotheses concerning their possible way of action. The high statistical significance of logP is certainly related to the membrane transport of these 1-tetrazolyl derivatives. Although steric and electronic properties have a much lower importance in comparison to hydrophobicity, we noticed that tetrazoles from this series are electron acceptors (E_{LUMO} values between -1.76 and -0.46 eV). This property is related to the electron transfer in different redox reactions. We suppose the algistic derivatives might substitute the membrane quinones, not tightly bound to the protein, implicated in the electron transfer in photosynthesis.

These quinones are the target of different herbicides.¹⁷ An AM1 calculation on the ubiquinone in Fig. 4, a potentially substitutable quinone, gives $E_{LUMO} = -1.48$ eV. Superposition of such a ubiquinone (with a short hydrophobic side chain) on the 3,4,5-Cl₃-phenyl and 5,6-Cl₂- β -naphthyl derivatives (derivatives IV and I, respectively from Table 5) can be seen in Figs. 4a and 4b. The ubiquinone from Fig. 4 superposes better on the potentially high active compounds than on any other molecule from the series.

Searching arguments for our hypothesis on the mechanism of action of algistic derivatives we find out the class 2 dihydroorotate dehydrogenases (DHODH) which are membrane-bound enzymes that use respiratory quinones as their physiological oxidants. One of the most prominent of their inhibitors is leflunomide (Arava). Its structure is displayed in Fig 5a. Using the optimized receptor map for model (3), MTD for leflunomide is 4 and logP 1.35. LogA calculated with model (3) is around 4.94. This value and the superposition of leflunomide on the most active molecule from the series displayed in Fig 5b suggest that leflunomide, has the necessary properties for a high algistic

activity. At the same time leflunomide's mechanism of action provides a solid argument for the validity of our hypothesis regarding the

mechanism of algistatic action of 1-aryl-tetrazoles from this series.

Table 3

Regression coefficients and the statistical data for the bi- and three-linear regressions; n=20

	Intercept (St. err)	logP (St. err)	q ₂ (St. err)	Dihedral, θ (St. err)	MTD (St. err)	r _{1,2}	r _{1,3}	r _{2,3}	R ²	SEE	F	q ² _{LOO}	SDEP
1	2.1502 (0.1442)	0.9250 (0.0884)		-0.0049 (0.0017)		0.04			0.872	0.197	57.94	0.809	0.223
2	1.4815 (0.1399)	0.9200 (0.0771)	-3.6092 (0.8880)			0.02			0.903	0.172	78.73	0.868	0.186
3	4.4602 (0.9209)	0.7797 (0.0465)			-0.1429 (0.0155)	-0.32			0.968	0.098	257.64	0.958	0.105
4	2.3213 (0.1361)	0.8059 (0.0439)		-0.0041 (0.0008)	-0.1219 (0.0155)	0.04	-0.34	0.11	0.974	0.092	198.24	0.968	0.096
5	2.9096 (0.1242)	0.8806 (0.0391)	-1.4879 (0.5316)		-0.1230 (0.0171)	0.02	-0.11	0.55	0.977	0.086	225.14	0.966	0.098

r_{1,2}, r_{1,3} and r_{2,3} – cross-correlation coefficients between descriptors of models (1) – (5); SDEP - the standard error of predictions

Table 4

Partial correlation coefficients of the scaled and orthogonalized descriptors used in models (4) and (5)

Model ID	Partial correlation coefficients			MTD significance
	logP	θ	MTD	
(4)	0.899	0.253	-0.319	electronic
(5)	0.899	0.307	-0.273	steric

Table 5

Structure, values of descriptors for five (I-V) potentially active tetrazoles and their estimated their logA using models (1) - (5)

	Substituents	logP	θ	q ₂	MTD1	MTD2	MTD3	1	2	3	4	5
I	1-(5,6-Cl ₂ -naphthalen-2-yl)-5-AT	3.1	42.84	-0.131	1	2	1	4.81	4.81	5.18	5.12	5.16
II	1-(5-Cl-naphthalen-2-yl)-5-AT	2.6	43.19	-0.132	2	3	1	4.34	4.35	4.65	4.68	4.63
III	1-(6-Cl-naphthalen-2-yl)-5-AT	2.6	43.23	-0.127	2	3	2	4.34	4.33	4.65	4.55	4.63
IV	1-(3,4,5-Cl ₃ -phenyl)-5-AT	2.6	43.23	-0.127	4	5	4	4.25	4.27	4.29	4.23	4.31
V	1-(3-Cl,4-OEt-phenyl)-5-AT	2.6	43.23	-0.127	3	4	3	3.59	3.52	3.88	3.7	3.86

5-AT – 5-aminotetrazole

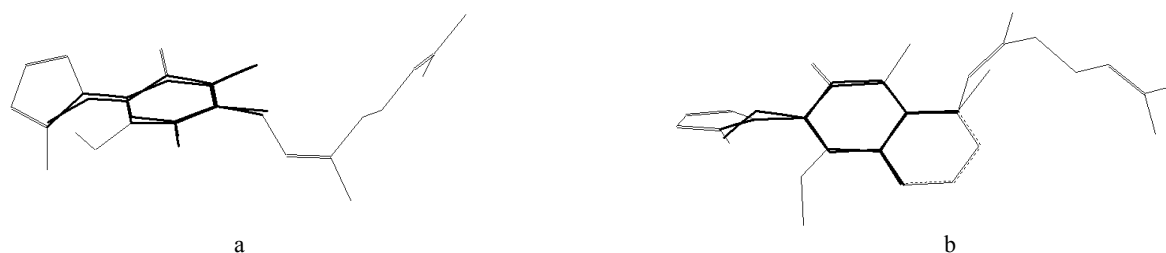


Fig. 4 – Superposition of an ubiquinone weakly bound to the membrane protein on a) 3,4,5-Cl₃ derivative (molecule IV, Table 5) and b) 5,6-Cl₂-naphthyl derivative (molecule I Table 5); thick lines represent the ubiquinone and tetrazole derivative's regions with maximum overlapping.

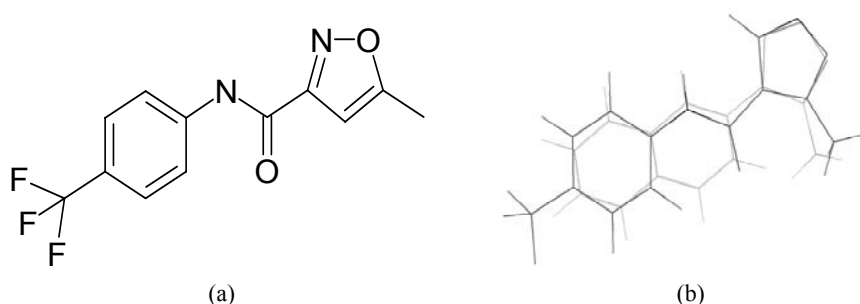


Fig. 5 – (a) Leflunomide structure and (b) leflunomide (thick line) superposition on the highest active molecule from the series (RMS fit 0.479 Å).

CONCLUSIONS

CoMFA and MTD methods applied to the series of 20 derivatives of 5-amino-1-aryl-1*H*-tetrazolyl lead to similar conclusions regarding the beneficial and detrimental regions of the aryl ring substituents.

The bi- and three-parameter regressions show that the algistatic activity of the 5-amino-1-aryl-1*H*-tetrazolyl derivatives is due to their hydrophobicity, and in a smaller degree to their steric and electronic properties. A probable mechanism of action of these tetrazolic derivatives is their transport to sites of quinones weakly bound to membrane protein, their binding at the easy substitutable quinone sites and the interruption of the chain of electron transfer in *Chlorella vulgaris* photosynthesis.

Acknowledgments: The authors thank to CNCSIS (Roumania) for allowing the financial backgrounds used for purchasing the HyperChem 7.52 package by CNCSIS grant nr. 776/2005.

REFERENCES

1. T. Schelenz, *J. Prakt. Chem.*, **2000**, 342, 205-210.
2. A. R. Katritzky, R. Jain, R. Petrukhin, S.N. Denisenko, T. Schelenz, *S. Q. Env. Res.*, **2001**, 12, 259-266.
3. R.D. Cramer, D.E. Patterson and J.D. Bunce, *J. Am. Chem. Soc.*, **1988**, 110, 5959-5967.
4. Z. Simon, "3D-QSAR in Drug Design. Theory, Methods, Applications", H. Kubinyi (Ed.), ESCOM, Leyden, **1993**, p. 307-319.
5. P. J. Goodford, *J. Med. Chem.*, **1985**, 28, 849-857.
6. H. Kubinyi, "Encyclopedia of Computational Chemistry Volume 1", P. Von Ragué Schleyer, N.L. Allinger, T. Clark, J. Gasteiger, P.A. Kollman and H.F. Schaefer III, (Eds.), New York, Wiley, **1998**, p. 448-460.
7. **Corina 1.8**, is available from Molecular Networks GmbH, www.molnet.de.
8. J. Sadowski and J. Gasteiger, *Chem. Rev.*, **1993**, 93, 2567-2581.
9. S. Wold, A. Ruhe, S. Wold and W.J. Dunn, *J. Sci. Stat. Comp.*, **1984**, 5, 735-743.
10. SYBYL™ and CoMFA are available from Tripos, Inc., www.tripos.com.
11. S. Wold, *Technometrics*, **1978**, 20, 397-405.
12. M.J.S. Dewar, E.G. Zoebisch, E.F. Healy and J.J.P. Stewart, *J. Am. Chem. Soc.*, **1985**, 107, 3902-3909.
13. *** HyperChem™, Release 7.52 for Windows, Copyright 2003, Hypercube, Inc, 1115 NW 4th Street, Gainesville, FL 32601, US.
14. R.G. Pearson, *Chemtracts-Inorg. Chem.*, **1991**, 3, 317-333.
15. L.H. Hall, B. Mahoney and L.B. Kier, *J. Chem. Inf. Comp. Sci.*, **1991**, 31, 76-80.
16. M. Randić, *New J. Chem.*, **1991**, 15, 517-525.
17. W. Draber, J.F. Kluth, K. Tietjen and A. Trebst, *Angew. Chem. Int. Ed. Engl.*, **1991**, 30, 1621-1633.

